Astronomy & Astrophysics manuscript no.
(will be inserted by hand later)

The "red shelf" of the Hβ line in the Seyfert 1 galaxies RXS J01177+3637 and HS 0328+05

P. Véron[1], A.C. Gonçalves[2] and M.-P. Véron-Cetty[1] ⋆

[1] Observatoire de Haute Provence, CNRS, F-04870 Saint-Michel l'Observatoire, France
e-mail: veron@obs-hp.fr; mira@obs-hp.fr
[2] European Southern Observatory (ESO), Karl Schwarzschild Strasse 2, D-85748 Garching bei München, Germany
e-mail: adarbon@eso.org

Received November 19, 2001; accepted January 9, 2002

Abstract. A few Seyfert 1s have a Hβ profile with a red wing usually called the "red shelf". The most popular interpretation of this feature is that it is due to broad redshifted lines of Hβ and [O III]$\lambda\lambda$4959,5007; we have observed two Seyfert 1s displaying a "red shelf" and showed that in these two objects the main contributor is most probably the He I $\lambda\lambda$4922,5016 lines having the velocity and width of the broad Hβ component. There is no evidence for the presence of a broad redshifted component of Hβ or [O III] in any of these two objects.

Key words. galaxies: Seyfert–galaxies: individual RXS J01177+3637, HS 0328+05

1. Introduction

A few Seyfert 1s have a very complex Hβ profile with a strong red wing extending underneath the [O III]$\lambda\lambda$4959,5007 lines. The excess emission in the red wing is referred to as the "shelf" feature or the "red shelf" (Meyers & Peterson 1985). In most Seyfert 1s showing such a feature, it appears to be made of two components: a broad red wing to Hβ, and a broad wing on the long wavelength side of the [O III]λ5007 line (van Groningen & de Bruyn 1989).

Several interpretations have been proposed to explain the "red shelf": it could be due to Hβ or to the presence of other broad emission lines such as [O III], Si II λ5056, He I λ5016 (Meyers & Peterson 1985; van Groningen & de Bruyn 1989; Kollatschny et al. 2001) or Fe II (Korista 1992).

Meyers & Peterson (1985), Crenshaw & Peterson (1986) and Stirpe et al. (1989) have argued that broad [O III] lines are most probably the main contributor to the observed λ5007 red wing. Van Groningen & de Bruyn (1989) have found the same red wing in [O III]λ4363 in several objects, confirming that they are indeed due to [O III] emission.

To investigate the nature of the "red shelf", we have made spectroscopic observations of two Seyfert 1s: RXS J01177+3637 and HS 0328+05.

2. Observations and data reduction

RXS J01177+3637 was observed on January 15, 1999, with the CARELEC spectrograph (Lemaître et al. 1989) attached to the Cassegrain focus of the OHP 1.93-m telescope. We obtained one 20 min exposure with a dispersion of 130 Å mm^{-1} in the range 4600 to 7900 Å. The detector was a 1024×2048, 13.5×13.5 μm pixel EEV CCD. Nine lines were extracted. The slit width was 2.″2 corresponding to 4.0 pixels on the detector; the resolution, as measured on the night sky lines, was ∼6 Å FWHM. The spectrum was flux calibrated with the standard stars EG 166 and EG 247 (Oke 1974) and Feige 66 (Massey et al. 1988).

In the case of HS 0328+05, the observations were carried out with the EMMI spectrograph attached to one of the Nasmyth foci of the ESO 3.58-m NTT telescope at La Silla. The detector was a 2048×2047, 24×24 μm pixel Tektronix CCD. Two spectra with a high signal-to-noise ratio (>50 in the continuum) were obtained, one in the red on November 24, 2000 (grism#6, 6000-8300 Å), the other in the blue on November 23 (grism#5, 4000-6600 Å). The exposure times were 30 and 45 min respectively. The slit width was 1″, corresponding to 3.7 pixels on the detector; the resolution, as measured on the night sky lines, was ∼ 4.5 Å FWHM. The nucleus was centered on the slit which was aligned with the parallactic angle. Seven lines were extracted. The spectra were flux calibrated with the stan-

Send offprint requests to: P. Véron

⋆ Based on observations obtained with the ESO NTT telescope, La Silla, Chile and the 1.93-m telescope at the Observatoire de Haute Provence (CNRS), France

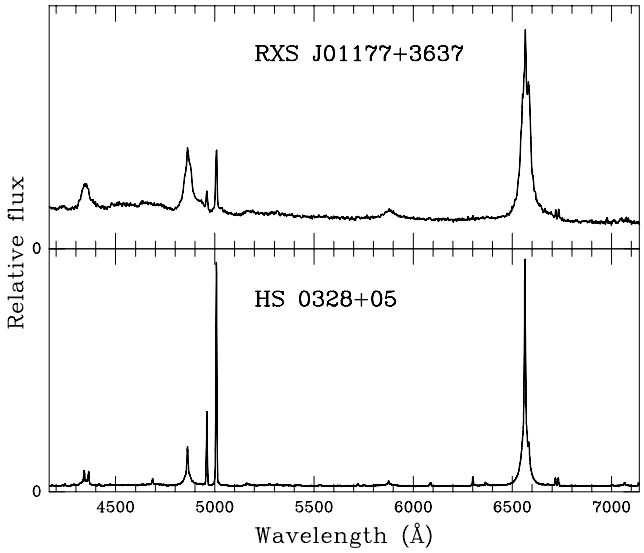

Fig. 1. Deredshifted spectra of RXS J011177+3637 and HS 0328+05.

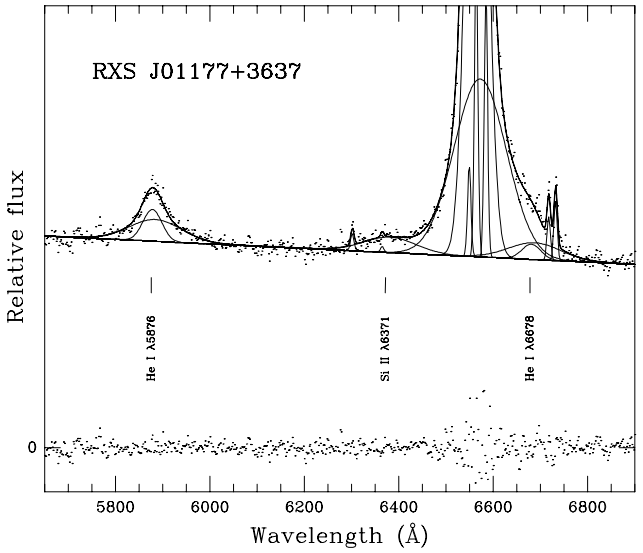

Fig. 2. Fit of the red part of the spectrum of RXS J01177+3637. The figure shows the data, the fit, the individual components and the residuals.

dard stars LTT 2415, LTT 3218 and LTT 9491 taken from Hamuy et al. (1992, 1994).

The spectra of the two objects are shown in Fig. 1. All the following analysis was done using our own software (Véron et al. 1980).

3. Analysis

3.1. RXS J01177+3637

RXS J01177+3637 is a Seyfert 1 at z=0.106 (Wei et al. 1999). Our spectrum clearly shows the presence of the "red shelf" (Fig. 1).

In a first step the broad Hα line was fitted with two Gaussians; the first (G1) has a FWHM of 2 150 km s^{-1} and a velocity of 130 km s^{-1} (with respect to the narrow emission lines), while the second (G2) has a peak intensity of 24% of that of the first, a FWHM of 6 100 km s^{-1} and a velocity of 560 km s^{-1}.

The red part of the spectrum also shows broad He I lines: λ5876, λ6678, λ7065 and a line near λ6370. The three He I lines have the width of the narrower Hα component G1 (λ5876/Hα=4.1%, λ6678/Hα=2.0%; λ7065/Hα=2.6%; here the Hα flux is that of the G1 component. The ionization potentials of Si I, Si II and Si III are nearly identical to the ionization potentials of Fe I, Fe II and Fe III and therefore the Fe^+ and Si^+ zones should be virtually the same; consequently Si II lines are expected in objects with strong Fe II emission (Phillips 1978); in several Seyfert 1s, an emission feature near 5050 Å has been attributed to Si II λ5056 (Crenshaw& Peterson 1986); we therefore feel confident that the line observed at λ6370 is Si II λ6371; this line has the width of the broader Hα component G2 (λ6371/Hα=8.6%), while the He I λ5876 and λ6678 lines also have a broader component (λ5876/Hα=12% and λ6678/Hα=9.5%). Fig. 2 shows the result of the fit of the red part of the spectrum.

In a second step we removed the Fe II multiplets in the blue part of the spectrum following the method described by Boroson & Green (1992), using a Fe II template obtained by taking a high signal-to-noise spectrum of I Zw 1 (Véron-Cetty et al. 2001), an NLS1 showing strong narrow Fe II emission. The resulting spectrum still shows strong broad red wings to Hβ and λ5007 (Fig. 3).

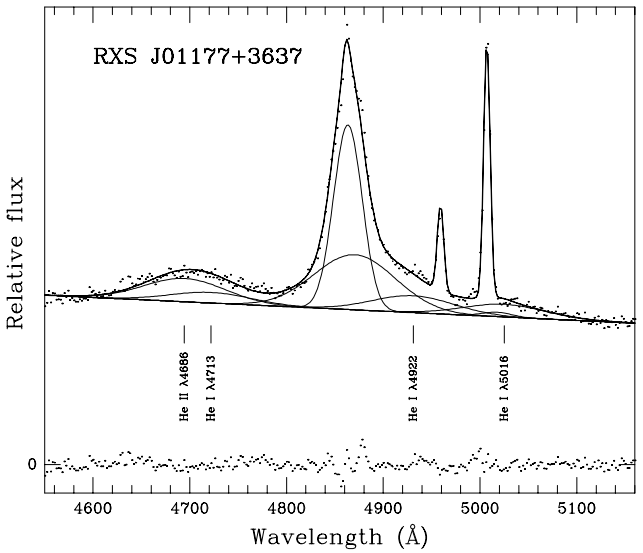

Fig. 3. Fit of the blue part of the spectrum of RXS J01177+3637. The figure shows the data (after subtraction of the Fe II emission), the fit, the individual broad components (Hβ, He I λ4713, λ4922 and λ5016 and He II λ4686) and the residuals.

We fitted the broad Hβ line with two Gaussian profiles having the velocities and widths of the Gaussian components (G1 and G2) of the broad Hα line. The broad red wings to Hβ and λ5007 are well fitted with broad (FWHM=6 100 km s^{-1}) Gaussian profiles (G2) at the wavelengths of He I λ4922 and λ5016 (λ4922/Hβ=30%; λ5016/Hβ=22%); the λ5016 line may also have a narrower (2 150 km s^{-1} FWHM) component (G1) with λ5016/Hβ=2.4%. The He II λ4686 and He I λ4713 lines are fitted each with a Gaussian profile with FWHM=6 100 km s^{-1} (G2); the He II line is very strong (λ4686/Hβ=42%); λ4713/Hβ=19% (Fig. 3).

Although higher quality spectra would be necessary to conclude unambiguously, it seems that the red wings to Hβ and λ5007 may be fully accounted for by the presence of the broad He I λ4922 and λ5016 lines respectively.

3.2. HS 0328+05

HS 0328+05 is a Seyfert 1 at z=0.043 (Perlman et al. 1996; Engels et al. 1998). The Balmer lines have been fitted with a broad Lorentzian profile with a FWHM of ∼1 500 km s^{-1} leading to the classification of this object as a NLS1; the Fe II emission was not detected, with the ratio of the Fe II emission measured between 4450 and 4684 Å and the total Hβ flux R_{4570} <0.6 (Véron-Cetty et al. 2001); our new high quality spectrum shows that Hβ has a weak, but definitively present, "red shelf"; in addition, the Fe II emission is detected with R_{4570}=0.43.

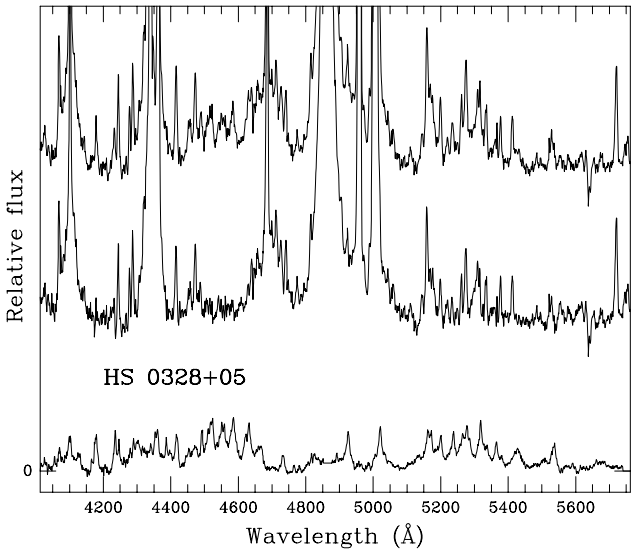

Fig. 4. The upper curve is the spectrum of HS 0328+05; the lower curve is the suitably scaled template Fe II spectrum; the middle curve is the difference (moved downward by an arbitrary amount for clarity). The quality of the iron removal is well seen in the spectral range 4450 to 4650 Å.

3.2.1. Narrow emission lines in the range 5080-5430 Å

In a first step we removed the broad Fe II multiplets as described above. In so doing we made the implicit assumption that the Fe II spectra of HS 0328+05 and I Zw 1 are identical; however according to Joly (1988) the relative intensities of the various multiplets are not the same in all objects, being a function of the temperature. Is then our assumption justified?

Inspection of the I Zw 1 Fe II spectrum (Fig. 4) shows that, in this object, the intensities of multiplets 25 (4846-5000 Å), 35 (5100-5180 Å) and 36 ($\lambda\lambda$4893,4993,5037) are quite small compared to that of m. 42 ($\lambda\lambda$4924,5018,5169), thus suggesting a temperature T_e > 8 000 K; if the temperature in HS 0328+05 were smaller (T_e < 7 000 K) the relative intensity of the first three multiplets would be much larger with respect to m. 42 (Joly 1988). Inspection of the residuals in Fig. 5 shows that the Fe II m. 35 has been completely cancelled out from the spectrum of HS 0328+05 by subtracting the template. It seems therefore that our procedure has indeed removed all the Fe II emission and that our initial assumption is justified.

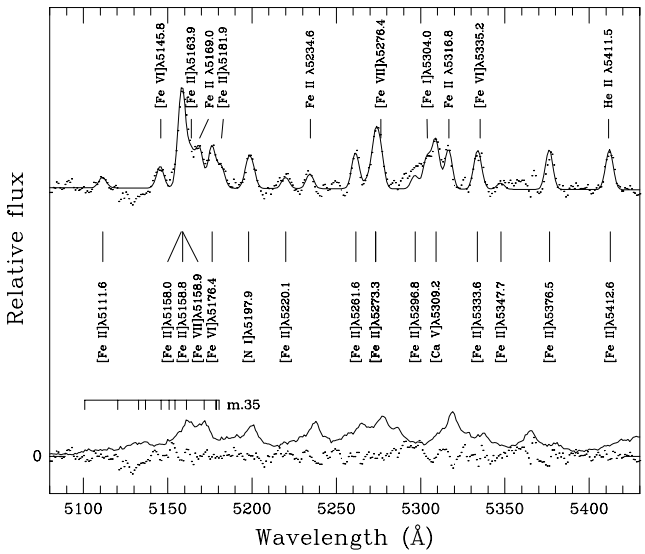

Fig. 5. Spectrum of HS 0328+05 (after subtraction of the broad permitted Fe II lines) in the range 5080 to 5430 Å. All identified emission features were included in the fit assuming that they all have the same velocity and width (namely 4.9 Å FWHM). Thirteen forbidden and three permitted Fe II emission lines are clearly detected. The bottom dotted line shows the residuals, while the solid line is the Fe II template subtracted from the original spectrum. The positions of the twelve lines in Fe II multiplet 35 are indicated.

The resulting spectrum is rich in narrow emission lines. We analysed a region free of broad emission features: 5080-5430 Å. Fig. 5 shows all the lines identified in this range including thirteen [Fe II] lines, three Fe II lines (λ5169

Table 1. [Fe II] lines observed in HS 0328+05. Col. 2 gives the multiplet numbers, col. 3 the radiative transition probabilities A (from Quinet et al. 1996), col. 4 the line intensities measured in the Orion nebula relative to He I λ6678, multiplied by 100 (Verner et al. 2000), col. 5 the relative intensities measured in HS 0328+05, col. 6 the log of the ratio of the intensities observed in HS 0328+05 and Orion.

λ_{lab} (Å)		A	I(Orion)	I(HS)	
4114.5	23F	0.103	0.25	0.30	0.08
4177.2	21F	0.194	0.26	0.23	−0.05
4244.0	21F	1.12	1.18	1.23	0.06
4276.8	21F	0.819	0.92	0.77	−0.08
4287.4	7F	1.65	2.32	1.58	−0.17
4319.6	21F	0.658		0.25	
4352.8	21F	0.380	0.51	0.45	−0.05
4358.4	21F	0.875		1.98	
4359.3	7F	1.22	1.60	1.36	−0.07
4372.4	21F	0.340		0.20	
4413.8	7F	0.858	1.16	0.82	−0.16
4416.3	6F	0.454	1.41	0.73	−0.28
4452.1	7F	0.548	0.90	0.53	−0.23
4457.9	6F	0.279	0.49	0.56	0.06
4474.9	7F	0.267	0.35	0.26	−0.13
4488.7	6F	0.150		0.55	
4639.7	4F	0.499		0.58	
4664.4	4F	0.156		0.18	
4728.1	4F	0.478	0.16	0.56	0.54
4774.7	20F	0.163	0.17	0.34	0.30
4814.5	20F	0.521	1.20	1.01	−0.07
4874.5	20F	0.223		1.16	
4889.6	4F	0.347	0.67	1.25	0.27
4905.3	20F	0.285	0.23	0.53	0.36
4947.4	20F	0.075	0.49	0.53	0.03
4950.7	20F	0.225	0.35	0.24	−0.16
4973.4	20F	0.183	0.36	0.17	−0.33
5020.2	20F	0.236		0.25	
5043.5	20F	0.094		0.49	
5111.6	19F	0.131	0.38	0.23	−0.22
5158.0	18F	0.440		0.62	
5158.8	19F	0.605	1.82	1.25	−0.16
5163.9	35F	0.309		0.67	
5181.9	18F	0.500		0.51	
5220.1	19F	0.144	0.15	0.27	0.26
5261.6	19F	0.429	1.36	0.68	−0.30
5268.9	18F	0.288	0.09	0.21	0.37
5273.3	18F	0.550	0.67	1.16	0.24
5296.8	19F	0.118	0.08	0.54	0.83
5333.6	19F	0.351	0.35	0.62	0.25
5347.7	18F	0.087		0.12	
5376.4	19F	0.348	0.46	0.78	0.23
5412.6	17F	0.283		0.63	
5527.3	17F	0.273		0.46	
5747.0	34F	0.373	0.08	0.49	0.79
7155.2	14F	0.153	1.50	0.99	−0.18
7172.0	14F	0.588	0.35	0.62	0.25
7388.2	14F	0.045	0.24	0.24	0.00
7452.5	14F	0.049	0.45	0.44	−0.01

(42), λ5234 (49) and λ5317 (48)), three [Fe VI] (2F) lines at λ5145.8, λ5176.4 and λ5335.2, and two [Fe VII] (2F) lines at λ5158.9 and λ5276.4.

The observed [Fe VI] lines have large predicted intensities (Garstang et al. 1978).

The two [Fe VII] lines $\lambda\lambda$5721,6087 (1F) are relatively strong with a ratio λ6087/λ5721=1.53, near the theoretical value of 1.60 (Nussbaumer & Storey 1982). According to Keenan & Norrington (1987), for densities lower than $\sim 10^6$ cm^{-3}, the intensity ratio λ5159/λ6087 is in the range 0.20-0.35. In the Seyfert 1 III Zw 77, Osterbrock (1981) has observed λ5159/λ6087=0.20. The two [Fe VII] lines λ5159 and λ5276 are blended with [Fe II] λ5159 (19F) and λ5273 (18F) respectively; we could however determine the intensity of [Fe VII]λ5276; assuming that the intensities of λ5276 and λ5159 are equal (their radiative transition probabilities are about equal, Keenan & Norrington 1987), we got λ5159/λ6087=0.2, confirming the identification of these two blended lines.

Having shown that the spectrum is dominated by [Fe II] lines, we looked for lines from this ion in the whole spectrum; the lines found are listed in Table 1 with their radiative transition probabilities and their relative intensities both in Orion when available (Verner et al. 2000) and HS 0328+05. These intensities are in good agreement (within a factor of 2), except for the weakest lines (I_{Orion} <0.25) for which our intensities are larger. A few of these lines were previously observed in the spectrum of NGC 4151 (Boksenberg et al. 1975). Several of them were not observed neither by Verner et al. (Orion) nor by Hamann (1994) (KK Oph); however their radiative transition probabilities computed by Quinet et al. (1996) are relatively large.

3.2.2. Fitting the spectrum around Hα and Hβ

We fitted the red spectrum (6250-6740 Å) with Gaussian components. The broad Hα is well fitted by three Gaussians H1, H2 and H3; their velocities are 51, –98 and 29 km s^{-1} respectively and their FWHM 1 730, 3 400 and 11 600 km s^{-1}. The relative peak intensity of these three components is 1.00, 0.40 and 0.04. The He I λ6678 line has a weak broad (1 730 km s^{-1} FWHM) component (H1), with λ6678/Hα=0.9%; broad lines (H1) of He I λ5876 and λ7065 are also present (λ5876/Hα=2.1%, λ7065/Hα=2.4%); λ5876 has also a broader (3 400 km s^{-1} FWHM) component (H2) with λ5876/Hα=5.5%. A broad (H1) line is required at λ6371 that we identify with Si II λ6371.

We showed in a preceding paper (Véron-Cetty et al. 2001) that the Balmer lines of NLS1s are better fitted with a single Lorentzian profile than with a single Gaussian profile. Our new high signal-to-noise spectrum shows that, at least in the case of HS 0328+05, this is not satisfactory and that a fit involving several Gaussians is

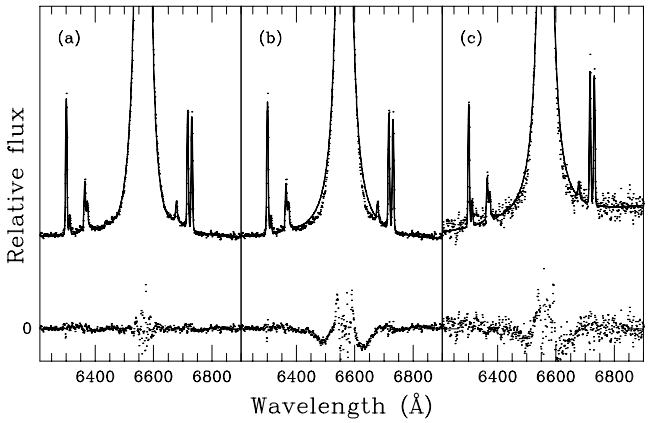

Fig. 6. Fit of the spectrum of HS 0328+05 in the range 6210 to 6900 Å. The broad Hα component has been fitted with three Gaussian profiles (a), with a single Lorentzian (b). (c) is the lower signal-to-noise ratio spectrum obtained with the OHP 1.93-m telescope fitted with a single Lorentzian. The high signal-to-noise reached with the NTT spectrum shows that the single Lorentzian fit is no longer acceptable.

needed (see Fig. 6).

We analysed in detail the blue spectrum in the range 4780 to 5120 Å which contains the Hβ and [O III] lines.

Fig. 7 shows the Hα profile superposed on the Hβ profile. The presence of an excess of emission in the red wings of Hβ and [O III]λ5007 is clearly visible. These broad emission features, centered at $\sim \lambda$4890 and $\sim \lambda$5050, are separated by a significant deep at $\sim \lambda$4980 suggesting that they are two distinct features.

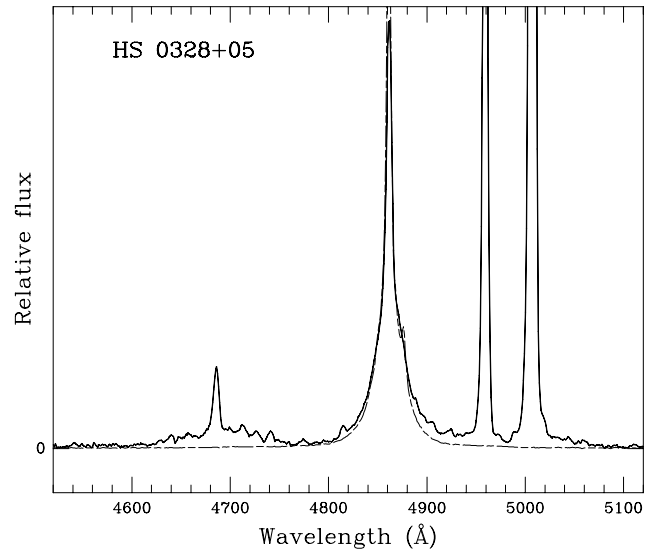

Fig. 7. The solid line is the blue spectrum of HS 0328+05 after subtraction of the Fe II emission; the dashed line is the Hα profile moved to the wavelength of Hβ. The excess of emission redward of Hβ is obvious.

We have divided the Hα profile by the Hβ profile; the Hα/Hβ ratio is $\sim$4 at the line center but drops quickly to $\sim$1 in the region of the red wing (4880-4940 Å), an unlikely value for the Balmer decrement. It seems therefore that the feature seen as a red wing to Hβ cannot be due to Hβ emission.

For the blue spectrum, we made a fit with Gaussian components including, for Hβ, two broad components having the velocity and FWHM of the two main broad components of Hα (H1 and H2); their intensity was let free; we found the Balmer decrement for these two components to be equal to 5.5 and 3.7 respectively. If the third, very broad, component (H3) had a Balmer decrement larger than three, it would not be detectable at Hβ.

We found necessary to include two broad Gaussian components to each of the He I lines λ4922 and λ5016, having the velocity and width of the narrowest broad Balmer profiles H1 and H2 respectively; their intensity with respect to the Hβ components is 8.1% and 3.8% respectively for H1 and 2.0% and 18.7% for H2.

We tried to identify all narrow lines in the range 4780 to 5120 Å. In addition to the [Fe II] lines listed in Table 1, we have identified two narrow permitted Fe II (42) lines: λ4924, λ5018, as well as [Fe VII] λ4893, λ4942 and λ4989, three lines in multiplet 2F with relatively large radiative transition probalities, and [Fe VI] λ4967 and λ4972 (2F), two lines with relatively strong predicted intensities (Garstang et al. 1978).

Several [Fe IV] lines have been observed in the spectrum of RR Tel (Thackeray 1954; Edlen 1969; Crawford et al. 1999); five of these lines (λ4868, λ4900, λ4903, λ4906 and λ4918), from the same multiplet a^4G-a^4F, are within the spectral range of interest and were included in our model, improving the fit.

We have identified the line [Ca VII]λ4940 which had previously been detected in the spectrum of RR Tel (Thackeray 1974; McKenna et al. 1997).

Our fit requires a line at λ4932.5 (λ4932/λ5007=0.003); Crawford (1999) observed a line at λ4930.5 in the spectrum of RR Tel and identified it with [O III]λ4931.0; however the three [O III] lines at λ5007, λ4959 and λ4931 are from a triplet originating from the same upper level; the transition probabilities are such that $\lambda4931/\lambda5007 = 9\times10^{-5}$ while the value observed in RR Tel is equal to 0.02, or 220 times larger than the theoretical value; we consider therefore that this line is unidentified.

We have found another unidentified line at λ4896.8. There is also a weak line at $\sim \lambda$5058; Si II λ5056 is not a good fit.

The narrow lines found in the range 4780 to 5120 Å are listed in Table 2. They were all included in our fit assuming that they have the same velocity and width (4.9 Å FWHM).

Table 2. Narrow emission lines identified in the range from 4780 to 5120 Å . Col. 1: line identification, col. 2: laboratory wavelength, col. 3: relative observed intensity in HS 0328+05, col. 4: intensity in RR Tel (Crawford et al. 1999).

iden	λ_{lab} (Å)	I_{HS}	$I_{RR\ Tel}$
[Fe II] (20F)	4814.5	0.69	0.367
Hβ	4861.3	32.10	30.550
[Fe IV]	4868.0	0.55	0.115
[Fe II] (20F)	4874.5	0.95	0.088
[Fe III] (2F)	4881.0	0.67	0.039
[Fe II] (4F)	4889.6	1.36	0.189
[Fe VII] (2F)	4893.4	0.21	1.250
?	4896.8	1.08	
[Fe IV]	4900.0	0.27	0.056
[Fe IV]	4903.5	0.32	0.068
[Fe II] (20F)	4905.3	0.49	0.145
[Fe IV]	4906.7	0.75	0.185
[Fe IV]	4918.1	0.32	0.078
He I (48)	4921.8	0.13	0.185
Fe II (42)	4923.9	0.98	0.128
?	4932.5	0.88	0.873
[Ca VII] (1F)	4940.3	1.02	3.063
[Fe VII] (2F)	4942.5	0.43	2.472
[Fe II] (20F)	4947.4	0.67	0.039
[Fe II] (20F)	4950.7	0.32	0.056
[O III] (1F)	4958.9	91.00	22.390
[Fe VI] (2F)	4967.1	0.65	0.579
[Fe VI] (2F)	4972.5	0.75	0.719
[Fe II] (20F)	4973.4	0.22	
[Fe VII] (2F)	4988.6	0.54	1.854
[O III] (1F)	5006.8	273.00	39.360
He I (4)	5015.7	0.75	0.328
Fe II (42)	5018.4	0.70	0.180
[Fe II] (20F)	5020.2	0.34	0.086
[Fe II] (20F)	5043.5	0.38	0.031
?	5058.0	0.40	
[Fe II] (19F)	5111.6	0.30	0.114

In the range 4915 to 4955 Å the emission excess is well fitted by a number of narrow emission lines ([Fe IV]λ4918, He I λ4922, Fe II (42) λ4924, [Ca VII] λ4940, [Fe VII]λ4942, [Fe II] (20F) $\lambda\lambda$4947,4951 and an unidentified line at λ4932.5 and by the broad components of He I λ4922 (see Fig. 8). We also find no need for a broad redshifted component to the [O III] lines.

4. Results and discussion

4.1. He I λ4922 and λ5016

Broad He I emission lines are observed in AGNs: λ3188 (Baldwin et al. 1980), λ4471 (van Groningen & de Bruyn 1989; Feldman & MacAlpine 1978), λ5876 and λ7065 (Feldman & MacAlpine 1978; Morris & Ward 1988) and λ10830 (LeVan et al. 1984). The He I lines at λ4471, λ4922, λ5016, λ5876 and λ6678 have been detected in the NLS1 galaxy Mark 110 (Kollatschny et al. 2001).

The broad He I λ4471 line is usually weak in Seyfert 1s (λ4471/λ5876$\sim$0.1) implying $n_e \sim 10^9$ cm^{-3} (Feldman & MacAlpine 1978; Almog & Netzer 1989).

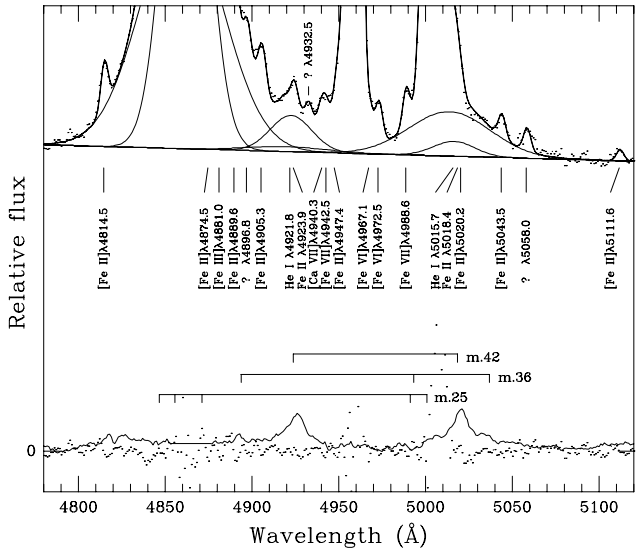

Fig. 8. Fit of the spectrum of HS 0328+05 in the range 4780 to 5120 Å. The figure shows the data (after subtraction of the Fe II emission), the fit and the broad individual components (Hβ and He I $\lambda\lambda$4922,5016). A number of narrow emission lines have been identified, many of them being due to iron. The "red shelf" is well fitted by a combination of narrow lines and broad He I λ4922 and λ5016 components. The bottom solid line shows the Fe II spectrum subtracted from the original spectrum while the dotted line shows the residuals.

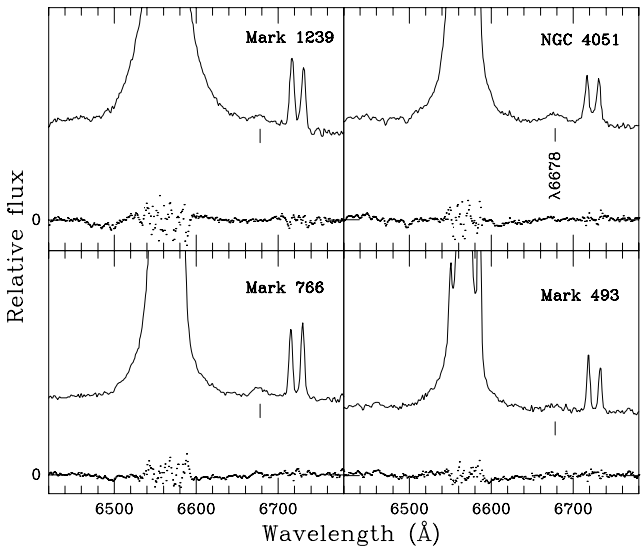

Fig. 9. The He I λ6678 line observed in four NLS1s galaxies

Van Groningen & de Bruyn (1989) concluded that the λ5016 line emission could contribute only a small fraction of the "red shelf" observed in Seyfert 1s; this statement was based on the assumption that λ5016 should not be stronger than λ6678 and that the strength of this last

line is typically 0.6-0.8% of that of Hα. Erkens et al. (1997) have however observed broad λ6678 in a number of Seyfert 1s with an intensity relative to Hα in the range 1.2-7.2%. We have detected this line in several NLS1s with an intensity relative to Hα in the range 0.8-2.6% (Mark 1239: 0.8%; NGC 4051: 2.6%; Mark 766: 1.7%; Mark 493: 1.2%) (see Fig. 9).

In the case of Mark 110, Kollatschny et al. (2001) convincingly showed that the red wing of [O III]λ5007 is due to a broad He I λ5016 line.

In the spectrum of RXS J01177+3637 and HS 0328+05, we have found He I lines emitted by the two broad Balmer line emission clouds; their relative intensities are listed in Tables 3 and 4.

In the case of HS 0328+05, we can set an upper limit to the intensity of a broad λ4471 component corresponding to λ4471/λ5876=0.15.

Table 3. Intensity relative to Hα of the He I lines observed in the spectrum of RXS J01177+3637

	FWHM (km s^{-1})	
	2150	6100
λ (Å)	I	I
4713		6%
4922		10%
5016	1.8%	7%
5876	4.1%	12%
6678	2.0%	9%
7065	2.6%	

Table 4. Intensity relative to Hα of the He I lines observed in the spectrum of HS 0328+05

	FWHM (km s^{-1})	
	1 730	3 400
λ (Å)	I	I
4922	2.7%	1%
5016	1.1%	6%
5876	2.1%	5%
6678	0.9%	
7065	2.4%	

At very high densities ($n_e > 10^{13}$ cm^{-3}), the He I lines may become very strong relative to the Balmer lines (Stockman et al. 1977); the Fe II emission region has a density which can almost reach this value ($10^{10} < n_e < 10^{11}$-10^{12} cm^{-3}) (Collin-Souffrin et al. 1980, 1988; Kwan et al. 1995).

4.2. Hβ wing

The wing to the red of Hβ has often been assumed to be Hβ emission coming from the same region as the [O III] wings with a low λ5007/Hβ ratio (close to unity) implying a relatively high density (10^7-10^8 cm^{-3}) (Meyers & Peterson 1985; van Groningen & de Bruyn 1989). Van Groningen & de Bruyn (1989) found no evidence for major differences between the Hβ and Hγ profiles in a number of Seyfert 1s; they also found that the wings detected on the long wavelength side of the [O III] lines have a clear counterpart in the Balmer lines.

However, although the broad Hβ line in Akn 120 has a red wing, the other Balmer lines do not show such a feature which, consequently, must be due to elements other than hydrogen (Foltz et al. 1983; Doroshenko et al. 1999).

In the spectra of RXS J01177+3637 and HS 0328+05, neither Hβ nor the [O III] lines have a broad redshifted component.

5. Conclusion

The detailed study of the spectrum of two Seyfert 1s showing a "red shelf" shows that it is mainly due, in addition to the Fe II multiplet 42, to the presence of relatively strong He I λ4922 and λ5016 broad lines. In HS 0328+05, there is also a non negligible contribution to the Hβ red wing of a number of narrow emission lines.

There is no evidence for the presence of a broad redshifted component in Hβ or [O III] in any of these two objects.

References

Almog Y. & Netzer H. 1989, MNRAS 238,57

Baldwin J.A., Carswell R.F., Wampler E.J. et al. 1980, ApJ 236,388

Boksenberg A., Shortridge K., Allen D.A. et al. 1975, MNRAS 173,381

Boroson T.A. & Green R.F. 1992, ApJS 80,109

Collin-Souffrin S., Dumont S., Heidman N. & Joly M. 1980, A&A 83,190

Collin-Souffrin S., Hameury J.-M. & Joly M. 1988, A&A 205,19

Crawford F.L., McKenna F.C., Keenan F.P. et al. 1999, A&AS 139,135

Crenshaw D.M. & Peterson B.M. 1986, PASP 98,185

Doroshenko V.T., Sergeev S.G., Pronik V.I. & Chuvaev K.K. 1999, Astr. Letters 25,569

Edlen 1969, MNRAS 144,391

Engels D., Hagen H.-J., Cordis L. et al. 1998, A&AS 128,507

Erkens U., Appenzeller I. & Wagner S. 1997, A&A 323,707

Feldman F.R. & MacAlpine G.M. 1978, ApJ 221,486

Foltz C.B., Wilkes B.J. & Peterson B.M. 1983, AJ 88,1702

Garstang R.H., Robb W.D. & Rountree S.P. 1978, ApJ 222,384

Hamann 1994, ApJS 93,485

Hamuy M., Walker A.R., Suntzeff N.B. et al. 1992, PASP 104, 533

Hamuy M., Suntzeff N.B., Heathcote S.R. et al. 1994, PASP 106, 566

Joly M. 1988, A&A 192,87

Keenan F.P. & Norrington P.H. 1987, A&A 181,370

Kollatschny W., Bischoff K., Robinson E.L., Welsh W.F. & Hill G.J. 2001, A&A 379,145

Korista K.T. 1992, ApJS 79,285

Kwan J., Cheng F.-Z., Fang L.-Z., Zheng W. & Ge J. 1995, ApJ 440,628
Lemaître G., Kohler D., Lacroix D., Meunier J.-P. & Vin A. 1989, A&A 228,546
LeVan P.D., Puetter R.C., Smith H.E. & Rudy R.J. 1984, ApJ 284,23
Massey P., Strobel K., Barnes J.V. & Anderson E. 1988, ApJ 328,315
McKenna F.C., Keenan F.P., Hambly N.C. et al. 1997, ApJS 109,225
Meyers K.A. & Peterson B.M. 1985, PASP 97,734
Morris S.L. & Ward M.J. 1988, MNRAS 230,639
Nussbaumer H. & Storey P.J. 1982, A&A 113,21
Oke J.B. 1974, ApJS 27,21
Osterbrock D.E. 1981, ApJ 246,696
Perlman E.S., Stocke J.T., Schachter J.F. et al. 1996, ApJS 104,251
Phillips M.M. 1978, ApJ 226,736
Quinet P., Le Dourneuf M. & Zeippen C.J. 1996, A&AS 120,361
Stirpe G.M., van Groningen E. & de Bruyn A.G. 1989, A&A 211,310
Stockman H.S., Schmidt G.S., Angel J.R.P. et al. 1977, ApJ 217,815
Thackeray A.D. 1954, Observatory 74,90
Thackeray A.D. 1974, MNRAS 167,87
van Groningen E. & de Bruyn A.G. 1989, A&A 211,293
Verner E.M., Verner D.A., Baldwin J.A., Ferland G.J. & Martin P.G. 2000, ApJ 543,831
Véron P., Lindblad P.O., Zuiderwijk E.J., Véron-Cetty M.-P. & Adams G. 1980, A&A 87,245
Véron-Cetty M.-P., Véron P. & Gonçalves A.C. 2001, A&A 372,730
Wei J.Y., Xu D.W., Dong X.Y. & Hu J.Y. 1999, A&AS 139,575